Journal of Traditional and Complementary Medicine 14 (2024) 568–580

Contents lists available at ScienceDirect

Journal of Traditional and Complementary Medicine

journal homepage: www.elsevier.com/locate/jtcme

Jintiange capsule ameliorates glucocorticoid-induced osteonecrosis of the femoral head in rats by regulating the activity and differentiation of BMSCs

Hui Xu [1], Lin Wang [1], Xunpeng Zhu, Haigang Zhang, Hongwei Chen, Hui Zhang [*]

Department of Orthopedics, The First Affiliated Hospital of Anhui Medical University, Hefei, China

ARTICLE INFO

Keywords:
Osteonecrosis of the femoral head (ONFH)
Glucocorticoids (GCs)
Bone mesenchymal stem cells (BMSCs)
Jintiange (JTG)
Differentiation

ABSTRACT

Background and aim: A surplus of glucocorticoids (GC) is a main cause of non-traumatic osteonecrosis of the femoral head (ONFH), and Jintiange (JTG), as one of the traditional Chinese medicines (TCM), also plays an instrumental role in the alleviation of bone loss simultaneously. Therefore, JTG was thought to be able to reverse GC-induced ONFH (GC-ONFH) to a certain extent.

Experimental procedure: In vivo, the effect of JTG on trabeculae in the subchondral bone of the femoral head was investigated using micro-computed tomography (micro-CT), TdT-mediated dUTP nick end labeling (TUNEL) and histological staining; in vitro, proliferation, viability, apoptosis, and senescence of purified bone mesenchymal stem cells (BMSCs) were examined to demonstrate the direct impact of JTG on these cells. Meanwhile after using a series of interventions, the function of JTG on BMSC differentiation could be assessed by measuring of osteogenic and adipogenic markers at levels of protein and mRNA.

Results: Our final results demonstrated that with the involvement of Wnt/β-catenin pathway, JTG was able to significantly promote osteogenesis, restrain adipogenesis, delay senescence in BMSCs, reduce osteoclast number, weaken apoptosis, and enhance proliferation of osteocytes, all of which could mitigate the progression of subchondral osteonecrosis.

Conclusion: According to the results of experiments in vitro and vivo, JTG was deemed to relieve the early GC-ONFH using the prevention of destruction of subchondral bone, which was contributed to regulating the differentiation of BMSCs and the number of osteoclasts.

1. Introduction

Osteonecrosis of the femoral head (ONFH) is characterized by joint pain and limited mobility, which can eventually lead to collapse of the femoral head and the need for total hip arthroplasty (THA).[1,2] Currently, there are between 500,000 and 750,000 reported cases of ONFH reported in China, with an increase of between 10,000 and 20,000 cases per year attributed to steroid use.[3,4] Glucocorticoids (GCs), such as methylprednisolone (MPS) and dexamethasone (DEX), are commonly used as first-line therapy in clinical practice for their anti-inflammatory and immunosuppressive effects.[5,6] However, as a double-edged sword, it has also been associated with a dramatic increase in the number of patients with glucocorticoid-induced ONFH (GC-ONFH), which has previously been reported to account for approximately 10–30% of cases of all atraumatic osteonecrosis cases in clinical practice.[2,7]

GC-ONFH is still the subject of various speculations regarding the specific mechanism, including fat embolism, vascular remodeling, abnormal coagulation, etc., and one of them is direct cells damage by GCs.[8,9] According to a number of studies, it is now well established that the side effects of GCs cause osteoblast-related cells to undergo apoptosis, resulting in a decrease in bone strength and mineral loss, ultimately leading to the collapse of subchondral bone in the femoral head.[8,10] The imbalance of differentiation induced by osteogenesis and adipogenesis may also contribute to the progression of GC-ONFH. Huang et al.[9] argued that excessive differentiation of adipocytes can increase pressure in the bone marrow cavity, cause a microvascular occlusion and reduce blood flow, and affect nutrient supply and inhibit bone formation and remodeling. What may become a crucial issue for the recognition of GC-ONFH is that bone-marrow mesenchymal stem cells (BMSCs), as progressives of bone cells, have naturally attracted extensive attention.

Peer review under responsibility of The Center for Food and Biomolecules, National Taiwan University.

* Corresponding author. Department of Orthopedics, The First Affiliated Hospital of Anhui Medical University, 218 JiXi Road, Hefei, Anhui, 230022, China.
E-mail address: zhanghui@ahmu.edu.cn (H. Zhang).

[1] The authors contributed equally to this work as co-first authors.

https://doi.org/10.1016/j.jtcme.2024.03.013
Received 12 September 2023; Received in revised form 26 February 2024; Accepted 5 March 2024
Available online 7 March 2024

Data from the recent work by Zhang et al.[7] suggested that GCs inhibit BMSC division and interfere with their normal differentiation process. According to Wang et al.,[11] GCs are also able to inhibit bone marrow renewal and accelerate its ageing, with osteogenic markers, such as runt-related transcription factor 2 (RUNX-2), showing a significant decrease, whereas adipogenic markers, such as peroxisome proliferator-activated receptors (PPAR-γ showed a significant increase. These conclusions once again highlight the critical role of BMSCs in GC-ONFH and provide new ideas for targeted treatment in the future.

In the absence of appropriate conservative management, approximately 70–80% of patients with ONFH will undergo THA.[12] Although THA is one of the most effective treatments for the end-stage ONFH, some patients still do not experience high clinical satisfaction due to limiting factors such as the length of time that the prosthesis lasts and complications that can occur during surgery.[13,14] As a result of its ability to relieve the pain caused by ONFH, traditional Chinese medicine (TCM), which consists of many ingredients, has been reported to be effective in improving quality of life to some extent.[15] Based on their clinical investigation, Li et al.[16] found that the Modified Qing'e Pill (MQEP) could reduce the risk of ONFH receiving THA by regulating bone metabolism and improving hypercoagulability. Similarly, Tetramethylpyrazine (TMP) was found to promote vascularization of the femoral head through the VEGF/FLK1 signaling pathway and inhibit the progression of ONFH in a rat study by Jiang et al..[17] A growing body of literature suggests that TCM containing bones from certain animals can effectively promote bone formation and inhibit bone resorption.[18]

The main component of the Jintiange (JTG) capsule is a type of biomimetic herbal medicine containing artificial tiger bone powder, which has been confirmed by basic research to be able to reverse cartilage degeneration and remodeling of subchondral bone in patients with osteoarthritis (OA).[19,20] According to JTG's previous review, the drug could increase levels of alkaline phosphate (ALP) and osteocalcin and reduce the activity of tartrate-resistant acid phosphate (TRAP) activity, suggesting it has the potential to improve trabecular bone structure by inhibiting bone resorption and promoting osteogenesis.[21] In addition, as a classical pathway of osteogenesis and adipogenesis, Wnt/β-catenin has been extensively documented in the mechanism of TCM and also plays a key role in the therapeutic processes of ONFH, suggesting that this pathway may be crucial in the treatment of ONFH.[22–24] Therefore, we believe that JTG may have some effect in alleviating GC-ONFH by stimulating the Wnt/β-catenin pathway.

Explicitly investigate the regulation of JTG on osteogenic (ALP and RUNX-2) and lipogenic (fatty acid binding protein 4, FABP-4 and PPAR-γ) related functions through activation of a Wnt/β-catenin pathway in the process of inhibiting the disease progression of GC-ONFH in vivo and in vitro, which will shed new light on an original treatment strategy for TCM treatment of early-stage GC-ONFH in the future.

2. Materials and methods

2.1. Isolation and culture of BMSCs

BMSCs were obtained from the femoral bone marrow of healthy, approximately 3-week-old SD rats, which were purchased from the Animal Experiment Center of Anhui Medical University. Briefly, a femur was separated under aseptic conditions and immersed in phosphate buffer solution (PBS; Beyotime, China). After Dulbecco's modified Eagle's medium (DMEM; Gibco, USA) was aspirated using a 1-mL syringe, the needle was inserted into the spongy bone, and the femoral medullary cavity was repeatedly strongly rinsed until the bone became white. In order to obtain BMSCs, the filtration liquid was centrifuged at 1500 rpm for 5 min after impurities were removed from the cell mixture with a marrow plug fitted with a 70 mm-mesh filter. Resuspended cells were incubated in 5 ml DMEM containing 15% fetal bovine serum (FBS; Gibco, USA) and 1% penicillin–streptomycin (Beyotime, China) in a 25 cm^2 flask (Thermo Fisher, USA) at 37 °C and 5% CO_2. Following the first seeding, the medium was replaced and the cells were cleaned three times with PBS, and then the medium was replaced every two days until the adherent cells reached 80–90% confluency. Further experiments were conducted using BMSCs from passages 3 to 6, and all details of the operating procedure were taken from previous research.[25]

For the purpose of verifying the efficacy of JTG (Purity >95%) obtained from Ginwa (Xi'an, China) and dissolved in PBS for suspension, cells will be treated with DEX (Solarbio, China), JTG, or both for a series of in vitro assays. The DEX concentration of 10 μM was selected to simulate the changes in the internal environment of the GC-ONFH as it will inhibit the proliferation and osteogenesis of BMSCs, which has been observed in previous studies.[2,10]

2.2. Cell viability assay

In accordance with the manufacturer's instructions, the Cell Counting Kit-8 (CCK-8) assay (APExBIO, USA) was used to assess the activity of cells and the toxicity of drugs. The BMSCs were plated into 96-well plates in triplicate at a density of 5×10^3 cells/well, and then incubated in 100 μL complete medium with 10 μM DEX and gradient concentrations of JTG (0, 5, 10, 20 mg/L) for different time. Following discarding the medium, 10 μL of CCK-8 buffer was added to BMSCs and incubated at 37 °C for 2 h at 1, 3, and 5 days. A microplate reader (Bio-Rad, USA) was used to measure the absorbance at 450 nm, and the difference in optical density (OD) ratio between the experimental group and the control group was calculated to assess the relative viability of the cells.

2.3. Cell proliferation assay

To determine whether DEX and JTG affect the proliferation of BMSCs, we used the EdU-594 Cell Proliferation Kit (Servicebio, China), and immunofluorescence was used to observe and analyze the results. To recap, BMSCs were incubated in 96-well plates at an initial density of $1x10^4$ cells/well for approximately 12 h with or without 10 μM DEX and 20 mg/L JTG.

After resuspended with 100 μL medium, BMSCs were incubated with 0.2 μL of EdU working solution at 37 °C for 2 h. At the back of PBS washing for twice, 4% paraformaldehyde (PFA; Beyotime, China) fixation for 15 min, and PBS washing for 2-3 times again, the cells were permeabilized with 0.5% Triton X-100 (Thermo Fisher, USA) for 15 min at room temperature, and finally washed with PBS to obtain labeled cells. The PBS was discarded and 100 μL of click additive solution was added to each well, which was incubated for 30 min at room temperature in the dark. An additional Hoechst staining (Servicebio, China) can be used to mark the nuclei and then observed with a Leica DM6B fluorescence microscope (Leica, Germany) after this procedure. Total cells (blue staining) and proliferating cells (pink and blue staining) were counted by randomly selecting five high-magnification visual fields.

2.4. Cell apoptosis assay

The Annexin V-FITC cell apoptosis detection kit (Beyotime, China) was used to verify the effect of JTG on BMSCs apoptosis according to the manual. Following 96 h of culture in FBS-free medium with or without 10 μM DEX and 20 mg/L JTG intervention, cells were digested, washed with PBS, and centrifuged prior to harvest. In the following step, cells were re-suspended in 200 μL of Annexin V-FITC solution and 10 μL of propidium iodide (PI) solution on an ice bath for 15 min in the dark. Then, the apoptosis ratio was obtained by analyses of flow cytometry, in which the characteristics of apoptotic cells were Annexin V- positive and PI is used to determine the stage of apoptosis.

2.5. Senescence cells histochemical staining assay

A senescence-associated β-galactosidase staining kit (Beyotime,

China) was used to verify the difference in the aging degree of BMSCs intervened or not by 10 μM DEX and 20 mg/L JTG. Following seeding on 6-well plates, the cells were washed once with PBS after 72 h of cell intervention and incubated with 1 mL of fixation buffer for 15 min at room temperature. After removing the buffer and washing three times with PBS, 1 mL of working solution was added to each well, which was then incubated at 37 °C and CO_2-free for one night with parafilm to prevent evaporation. Blue staining was visualized with an inverted microscope (Carl Zeiss, Germany) following the addition of PBS to halt the reaction, and statistical analysis of aging cells was performed using three high-fold images randomly selected.

Meanwhile, the detection of senescence-associated secretory phenotype (SASP, such as IL-6 and TNF-α) in BMSCs, which is another major indicator of cellular senescence, was verified by levels of mRNA. The main steps of this part are described in the section "Quantitative real-time polymerase chain reaction (qRT-PCR) analysis ".

2.6. Osteogenic and adipogenic induction

To induce differentiation of osteoblasts and adipocytes, BMSCs were cultured at the appropriate density on 6-well plates. Once 90% of the flask had been covered with cells, the normal medium (with or without 10 μM DEX and 20 mg/L JTG) was discarded and the complete osteogenic and adipogenic induction media (both from Cyagen, China) were applied under specific conditions according to the instructions. After 48 h of culture, the cells were collected for subsequent verification of the levels of protein and mRNA, respectively. The mineralized calcium and droplets for lipid were stained with Alizarin Red S and Oil Red O solution (both from Cyagen, China) after 21 days and 14 days of osteogenic and adipogenic induction, respectively, and the effect of JTG and DEX on different differentiation of BMSCs was assessed by measuring the size of the stained areas. Lastly, Axio Observer 3 inverted microscope (Carl Zeiss, Germany) was used for observation, and ImageJ software (national institutes of health, USA) was used for quantitative analysis of staining ratio by selecting three random high-magnification (× 400) fields in each group with respect to stained area ratio.

2.7. Western blot

Following induction of BMSCs from SD rats, the cell membrane was lysed in RIPA buffer (Beyotime, China) with a proteinase inhibitor for 30 min. Then, protein was detected and extracted, and the concentration of lysates was quantitatively determined by a BCA Kit (Beyotime, China). The denatured proteins were then electrophoresed on SDS-PAGE gels and transferred to polyvinylidene fluoride (PVDF) membranes after being denatured at 100 °C for 5 min. Membrane was sealed with 5% fat-free dried milk at room temperature for 1 h, and then appended with the primary antibodies of β-catenin, RUNX-2, ALP, PPAR-γ, FABP-4 and GAPDH (1:1000, all from Huabio, China) was incubated at 4 °C for the night, then immersed in horseradish peroxidase (HRP)-condensed secondary antibodies (1:1000, Huabio, China) at 37 °C for 1 h. After that, target bands were observed and imaged under Tanon 5200 chemiluminescence imaging system (Tanon, China).

For nuclear protein extraction, a Nuclear and Cytoplasmic Protein Extraction Kit was used (Beyotime, China). Briefly, the cytoplasmic protein extraction reagents (Reagent A and B) and nuclear protein extraction reagents were dissolved into 1 mM by Phenylmethanesulfonyl fluoride (PMSF; Beyotime, China) respectively and placed in ice for later use. After the separation of adherent cells by ethylene diamine tetraacetic acid (EDTA; Beyotime, China) and cell scrapers, cell precipitates were collected by centrifugation. This precipitate was resuspended in 200 μL of Reagent A and 10 μL of Reagent B, iced for 10 min, and centrifuged for 5 min at 4 °C after being resuspended in 200 μL of Reagent A and 10 μL of Reagent B. As a next step, 50 μL of nuclear protein extraction reagent was added to the precipitate after discarding the supernatant of cytoplasmic protein. Finally, the nuclear protein in the supernatant was verified by western blot to judge the content change of β-catenin in the nucleus.

All experiments will be repeated three times, and then the average gray level of the protein band will be quantitatively analyzed by ImageJ software.

2.8. Quantitative real-time polymerase chain reaction (qRT-PCR) analysis

To explore the transcriptional differences of osteogenic and adipogenic-related mRNAs, total RNA was obtained from the Trizol Reagent (Invitrogen, USA) and 1 μg of each group was transcribed using a primer RT Reagent Kit (Takara, China) to complete the cDNA synthesis according to the protocols. With GAPDH as the normal reference, PCR reactions of target genes (*Runx2*, *Alp*, *Pparγ*, *Fabp4*, *Il6* and *Tnfα*) were performed using CFX 96 Real-time PCR Detection System (Bio-Rad, USA) under the conditions as follows: 40 cycles of 95 °C for 15 s and 60 °C for 60 s after 5 min of inactivation at 95 °C. The primer sequences referred to above for amplification are presented in Table 1, and the quantitative analysis of the final gene expression was achieved by calculating values of $2^{-\Delta\Delta CT}$ as recorded previously.[26]

2.9. Animal model and grouping

A total of thirty healthy female Sprague-Dawley (SD) rats (8-weeks-old, weight about 250 g) were purchased from the Animal Experiment Center of Anhui Medical University, and all animal experiments and procedures have been approved by the Animal Research Ethics Committee of Anhui Medical University (Ethical Code: LLSC20231033). After acclimating for one week, all rats were randomly divided into three groups: (1) Control group (served with normal saline, n = 10); (2) MPS (Pfizer, USA) group (served with MPS, n = 10); (3) MPS + JTG group (served with MPS and JTG, n = 10). The rats were raised under the same environmental conditions, which included a constant temperature of 25 °C, 12 h of daily movement and adequate food and water.

The dosage, time and mode of MPS administration are similar to those described previously with appropriate modifications.[12,27] In short, SD rats of MPS group and MPS + JTG group were intraperitoneally injected with 0.2 mg/kg lipopolysaccharide (LPS; Sigma-Aldrich, USA) for one time in the first week, and then intramuscularly injected with 100 mg/kg large dosage of MPS for three consecutive days (three injections in all for each rat). From the second week, SD rats of two groups were given intramuscular injection of MPS at a maintenance dosage of 40 mg/kg three times a week for 5 weeks (fifteen injections in all for each rat) to prevent self-repair of femoral osteonecrosis, and at the same time, 360 mg/kg JTG was given to rats of JTG group every other day by intragastric administration until sacrifice in view of previous research.[28] The SD rats of the Control group consumed the same volume of normal saline (NS) at each stage. As a result of the treatment, all rats that were still alive after 6 weeks were killed, and then samples of femoral heads were harvested for analysis by micro-CT, histological/immunohistochemical staining, and related apoptosis tests were conducted.

Table 1
Primer sequences of genes in qRT-PCR.

Gene	Forward primer	Reverse primer
Runx2	CCGCCTCAGTGATTTAGGGC	GGGTCTGTAATCTGACTCTGTCC
Alp	ACCGCTTCCCATATGTGGCT	TGCACCAGATTCTTCCCGTC
Pparγ	CTTGCAGTGGGGATGTCTCAT	AGCAAACCTGGGCGGTTGAT
Fabp4	ACTGGGCCAGGAATTTGACG	CTCGTGGAAGTGACGCCTT
Il6	GACTTCCAGCCAGTTGCCTTCTT	TGGTCTGTTGTGGGTGGTATCCT
Tnfα	CTCATTCCTGCTCGTGGCG	CGTGGGCTACGGGCTTGT
Gadph	CCATGACAACTTTGGTATCGTGGAA	GGCCATCACGCCACAGTTTC

2.10. Micro-computed tomography (CT) scanning

The specimens were preserved at room temperature with 4% PFA, then scanned by SkyScan 1276 (Bruker, Germany) at a voxel of 9 μm and two-dimensional (2-D) images were observed by Data Viewer software (version 1.5.1.9, Bruker). A three-dimensional (3D) image was derived from contoured two-dimensional (2-D) images using methods based on distance transformation of the grayscale original images through processing with CTVox software (version 3.3.0, Bruker), and quantitative analysis of relevant bone parameters as below was performed by CTAn software. (version 1.18.8.0, Bruker): bone mineral density (BMD), percent bone volume (BV/TV), bone surface/volume ratio (BS/BV), bone surface density (BS/TV), trabecular pattern factor (Tb.Pf), structure model index (SMI), trabecular thickness (Tb.Th) and trabecular separation (Tb.Sp). The region of interest (ROI) was selected in the area of subchondral bone of the femoral head according to previous reports.[10,29]

2.11. Histological, immunohistochemical (IHC) and immunofluorescence (IF) analyses

After decalcification with 10% EDTA (PH = 7.4) and paraffin embedding, the femoral head was sectioned at 5-μm thickness along the coronal plane. Upon deparaffinization with xylene, ethanol hydration with decreasing concentrations, and rinsing with distilled water, staining tests were applied to the tissue sections as follows: (1) Hematoxylin and eosin (H&E; Servicebio, China) staining was used to identify the distribution of marrow oedema, marrow fat and empty lacunae; (2) Tartrate-resistant acid phosphatase (TRAP; Servicebio, China) staining was applied to calculate osteoclast number/bone surface (N.Oc/BS); (3) Goldner's Trichrome (Servicebio, China) staining was employed to judge the mineralized area of calcified bone.

As to IHC staining, anti-ALP, RUNX-2 (both at the dilution of 1:200, Huabio), were used to determine the osteogenesis and expression level of adipose cell-related protein was test by anti-PPAR-γ, FABP-4 (both at the dilution of 1:100, Huabio). The details of the incubation were the same as the part of the western blot above.

All stained tissue sections were observed with a Leica microscope (Leica, Germany), and five high-magnification microscope fields were randomly selected from each sample of subchondral bone for quantitative calculation with the help of ImageJ software.

2.12. TdT-mediated dUTP nick end labeling (TUNEL) assay

An apoptosis assay kit based on the TUNEL method (Beyotime, China) was used to detect apoptosis in tissue after a series of steps such as decalcification, embedding, slicing, and dewaxing (Beyotime, China). After washing in PBS, the sectioned tissues were incubated with protease K without DNase at room temperature for 15 min, followed by blocking and incubation for 1 h in the presence of 100 μL of TUNEL reaction solution at 37 °C in the dark. The number of TUNEL-positive cells (green cells) and the total number of cells (blue cells) were counted and analyzed under the LSM-880 confocal microscope (Carl Zeiss, Germany) through five randomly selected high-magnification images from the parts of subchondral bone.

2.13. Statistical analysis

Statistical analysis was performed on Statistical Product Service Solutions (SPSS) software (version 25.0, IBM-SPSS) and the graphics were produced on Graphpad Prism (version 8.0, Graphpad Software). Data conforming to the normal distribution were presented as mean ± standard deviation (SD) and a one-way analysis of variance (ANOVA) test was used to compare these data among multiple groups. $p < 0.05$ was considered statistically significant and all experiments used for statistics were repeated at least three times.

3. Results

3.1. Effects of JTG on viability and proliferation of BMSCs induced with GC in vitro

The effects of JTG and DEX on the activity and proliferation of BMSCs were explored by a CCK-8 assay, a β-galactosidase assay and an EdU assay respectively. Based on the analysis of the CCK-8 data, one group indicated that the absorbance of BMSCs increased regularly in a time-dependent manner, whereas the absorbance of BMSCs treated with DEX alone was significantly inhibited in every period when compared with the control group, and JTG was able to significantly counteract this inhibitory effect in a dose-dependent manner ($p < 0.05$) (Fig. 2(I)). It is for this reason that the therapeutic dose in subsequent vitro studies will be calculated using a concentration of JTG of 20 mg/L. On the other hand, it was found in a β-galactosidase staining assay that there was obvious accumulation of aged BMSCs in DEX group (10.18%), and the proportion of aging decreased significantly in response to the treatment of JTG (1.83%) and in Control (0.47%) (Fig. 1(C, H)); Similarly, mRNA levels of IL-6 and TNF-α of SASP were significantly higher in the DEX group than in the Control group and the DEX + JTG group($p < 0.05$, Fig. 1 (D, E)). According to the fluorescent staining results obtained from an EdU assay, the percentage of BMSCs treated with DEX exhibited a decrease in proliferation, whereas JTG-treated BMSCs displayed an opposite trend (0.63% vs 3.23%, $p < 0.05$) (Fig. 1(B, G)).

There was consensus among these studies that GC could directly impact the proliferation activity and aging rates of BMSCs, and that JTG could effectively mitigate these adverse effects.

3.2. Effects of JTG on cell apoptosis intervened with GC in vitro and in vivo

In vitro, the apoptosis of BMSCs was judged by Annexin V/PI double staining and counted using flow cytometry. After starvation-induced culture under different conditions, the average proportion of apoptotic BMSCs dramatically increased to 17.27% after DEX interference. Nevertheless, when JTG was added to BMSCs that had been disturbed by DEX in addition, the proportion of apoptosis decreased to 6.52% ($p < 0.001$) (Fig. 1(A, F)). An in vivo TUNEL assay confirmed this perspective, finding that the number of positive apoptotic cells in BMSCs from JTG + MPS-treated subjects was significantly lower than that in MPS-treated subjects (50.6% vs 15.27%, $p < 0.001$) (Fig. 5(A, E)).

Research conducted in the aforementioned studies has provided strong evidence that JTG can effectively suppress the side effects of GC on the induction of apoptosis in the subchondral bone tissue of the femoral head.

3.3. Effects of JTG on osteogenesis and adipogenesis treated with GC in vitro and vivo

Following BMSC differentiation under various conditions, Alizarin red S and Oil red O staining were used to determine the degree of differentiation, which was then assessed in vitro by measuring the expression of representative mRNAs and proteins (Fig. 2(A-C)). BMSCs treated with JTG increased the staining area of calcium nodules while decreasing lipid droplets significantly as compared to those treated with DEX alone, which was also confirmed at the protein and mRNA levels by western blot and qRT-PCR experiments following osteogenic (ALP and RUNX-2) and adipogenic (PPAR-γ and FABP-4) inductions, respectively (Fig. 2(D, F, G)). The above-mentioned phenomena were reappeared in IHC staining in vivo as well, that is, the expression levels of ALP and RUNX-2 in JTG-treated specimens were opposite to those of FABP-4 and PPAR-γ remarkably (Fig. 4). The involvement of the Wnt/β-catenin pathway in the progression of GC-ONFH was verified by Western blot. The expression levels of β-catenin protein in cells and nuclei after JTG treatment were both significantly increased, while the decrease in

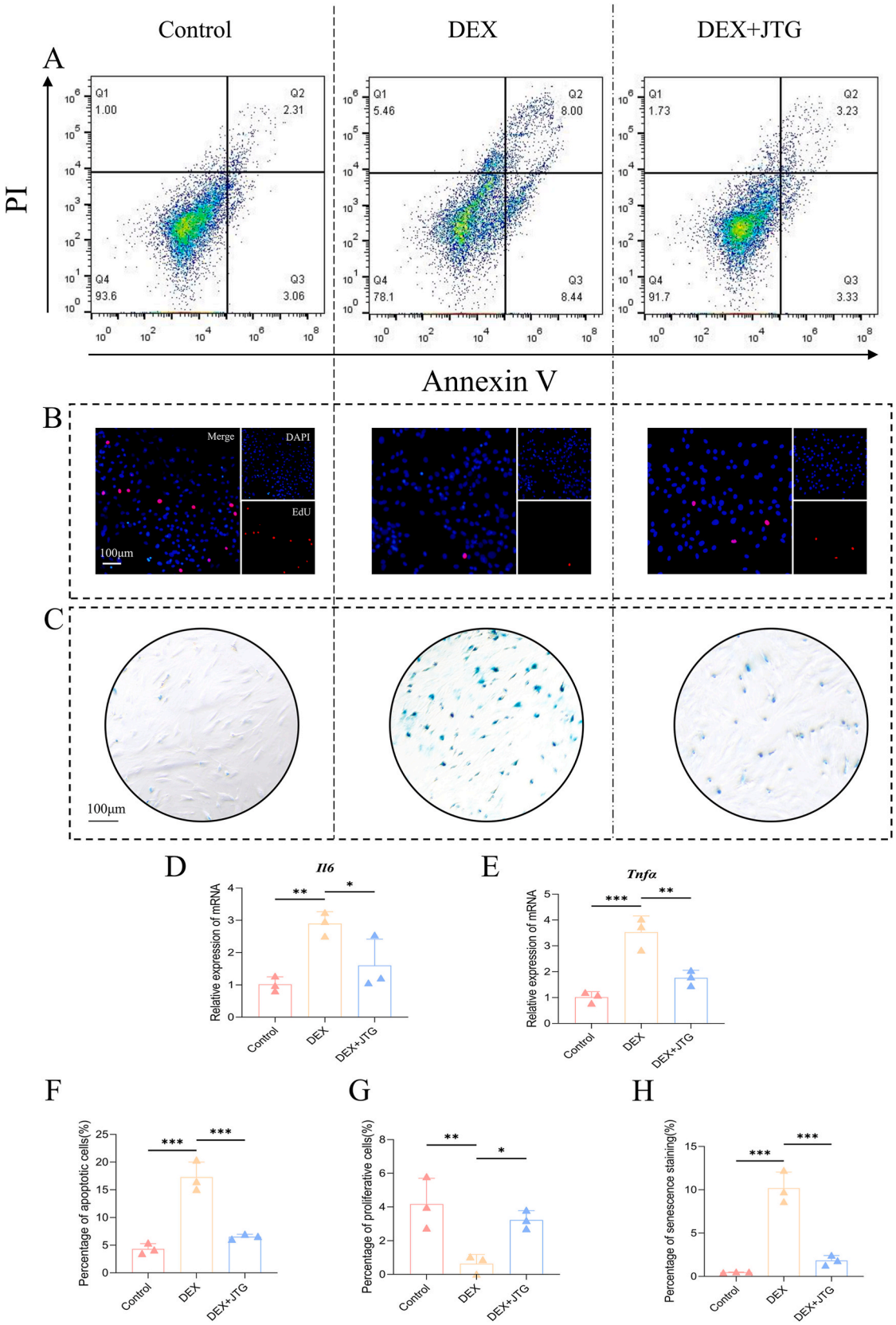

Fig. 1. Flow cytological examination, EdU immunofluorescence and β-galactosidase staining of BMSCs in rats. A) Flow cytometry results indicated that JTG was able to weaken the cytotoxicity of DEX at the cellular level. B) EdU staining determined that the proportion of proliferating cells increased significantly in the DEX + JTG group compared to the DEX group. C) β-galactosidase staining demonstrated that JTG significantly reduced the proportion of senescent cells in the GC-ONFH microenvironment. D-E) qRT-PCR results suggested that JTG could significantly reduce the transcription of SASP (IL-6 and TNF-α) from senescent cells. F-H) Quantitative analyses of each assay were represented as the mean ± SD (n = 3 per group, $p < 0.05$; *$p < 0.01$; ***$p < 0.001$ relative to the DEX group).

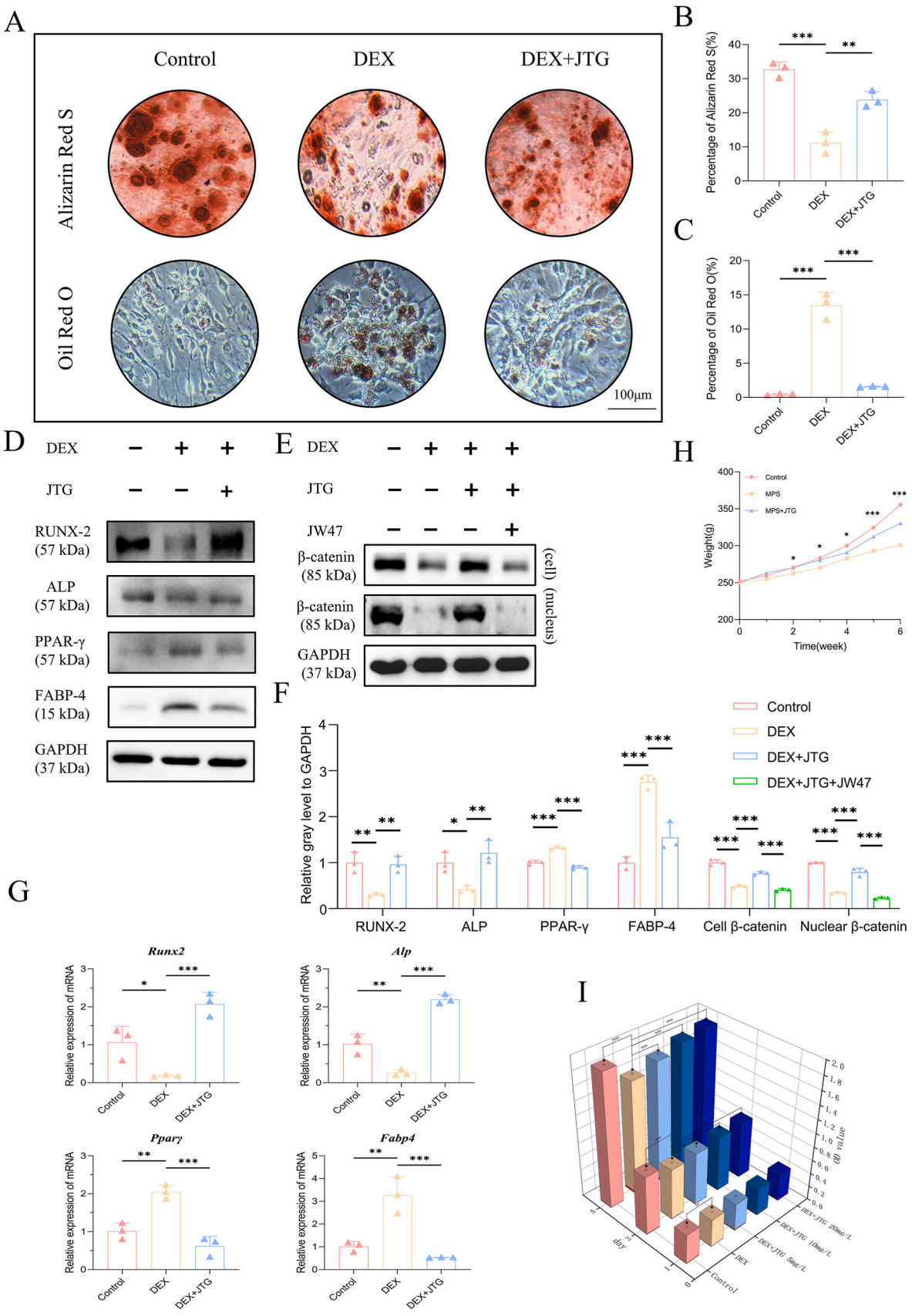

(caption on next page)

Fig. 2. Staining for induction of osteogenesis and adipogenesis and expression levels of proteins and mRNA after induction, changes in body weight in rats at different stages and detection of CCK-8 cells activity. A) Alizarin Red S and Oil Red O staining indicated that JTG interfered with the differentiation of BMSCs by promoting osteogenesis (red calcium nodules) and inhibiting adipogenesis (red lipid droplets). B-C) Quantitative analyses of the ratio of staining and presented as the mean ± SD (n = 3 per group). D-F) Western blot and quantitative analysis (n = 3 per group) indicated that JTG stimulates osteogenic protein synthesis and inhibits lipoprotein synthesis by activating the Wnt/β-catenin pathway. G) Quantitative analyses of expression of mRNA in each protein and reported the mean ± SD (n = 3 per group). H) Weighing results revealed that the MPS intervention would result in a significant reduction in rats' weights, whereas the JTG intake would alleviate the weight loss in rats. The data were represented as the mean ± SD (n = 6 per group). I) It is evident from the absorbance measurements of CCK-8 that DEX significantly reduced the activity of BMSCs and that JTG alleviated the adverse effects of such conditions to a varying extent, depending on its concentration. The data were represented as the mean ± SD (n = 3 per group). (*$p < 0.05$; $p < 0.01$; *$p < 0.001$ relative to the DEX/MPS group).

protein level after the addition of the 1 μmol/L of Wnt antagonist JW74 (MedChemExpress, USA), concentration was determined from previous experiments,[30] in BMSCs co-treated with JTG and DEX verified the key role of Wnt/β-catenin pathway in GC-ONFH once again (Fig. 2(E, F)).

These studies indicated that GC could influence BMSC differentiation through blocking osteogenesis and increasing adipogenesis, while JTG could effectively reverse this detrimental tendency.

3.4. Effects of JTG on alleviating GC-ONFH in the rat model

As a result of the adaptive feeding period, the rats' spirits and appearance were normal in all three groups and there was no significant difference between them. Upon commencing the drug injections, rats in the MPS group displayed languid symptoms, including yellowish hair, loss of luster, and alopecia. With continual administration of GC, rats gradually lost weight and became malnourished, eventually dying. Upon receiving a gavage dose of JTG, rats were able to regain some of their physical appearance and mental state. Even though some of the rats in the MPS + JTG group died as a result of operation problems, measurements of their systemic status, such as their body weight, showed a marked improvement (Fig. 2(H)).

Six weeks later, all the femoral heads were extracted and scanned by micro-CT. A 2-D plane and 3-D reconstruction indicated that trabecular bone was sparse in the subchondral part of femoral heads in the MPS group, while necrotic areas were evidently reduced in the MPS + JTG group (Fig. 3(A)). In a quantitative analysis of bone trabecula, these visual presentations were supported by the comparison of various parameters (Fig. 3(B)).

To facilitate further staining tests, paraffin sections of the scanned specimens were made after undergoing a series of steps. Evidence of HE staining was found in the tissue of MPS group, with an increase in the proportion of lacunae that were empty (15.56% vs 67.11% vs 23.56%, both $p < 0.001$ for MPS group) (Fig. 5(B, F)). In the interim, Goldner's Trichrome and TRAP staining showed that the mineralization degree of sections in this group decreased (78.9% vs 55.4% vs 71.02%, both $p < 0.01$ for MPS group) but the distribution density of osteoclasts increased to the contrary (0.37% vs 2.08% vs 0.58%, both $p < 0.001$ for MPS group), which was in agreement with the aggravation of GC-ONFH. When supplemented with JTG, the performance of accelerating the deterioration degree of GC-ONFH was significantly improved (Fig. 5(C, D, G, H)).

As discussed above, these findings confirmed that: on the one hand, MPS has been successfully applied to the establishment of GC-ONFH models; on the other hand, JTG inhibits the apoptosis of osteocytes, reduces the number of osteoclasts and increases bone mineralization in rat models of GC-ONFH.

4. Discussion

In terms of acquired non-traumatic ONFH, alcohol and steroids were the two most prominent triggers.[31] Current research suggests that alcohol-induced ONFH may be caused by a similar mechanism to that of GC, in that the substance leads to abnormalities in the differentiation and activity of BMSCs, as well as impairing bone resorption and remodeling.[30,32] In a study conducted by Yu et al.,[33] Chrysophanic acid, as a type of TCM, was found to inhibit the progression of alcohol-induced ONFH by regulating the differentiation trend of BMSC differentiation trend, which is consistent with the findings of this study.

Bone remodeling is a lifelong process by fine-tuning the differentiation tendencies in BMSCs, leading to the formation of osteoblasts and the resorption of bone by osteoclasts.[34] In addition to causing fat accumulation and delaying ossification, increasing evidence suggests that GC-ONFH is associated with osteoclast lifespan extension and direct apoptosis of BMSCs and osteoblasts.[12,34,35] There is currently no effective treatment for the specific cause of the condition, and a number of emerging non-surgical treatments have limitations that prevent their widespread use in the clinic.[14,36] The most promising of these was stem cell therapy based on the vitality and secretory function of BMSCs, which showed promising results, particularly in hip preservation therapy for young and middle-aged patients.[37,38] It is noteworthy that stem cell therapy offers a number of advantages over traditional THA, including minimal invasiveness and the ability to preserve function, but its long-term effects and safety remain controversial, suggesting that many difficulties remain before the method can be flexibly applied to standardized treatment.[14] With this in mind, there is still much room for further research into more effective treatment options for early GC-ONFH.

In TCM, raw materials derived from Chinese animals are combined with herbs in specific proportions according to a recipe or traditional theory.[39,40] Numerous publications have documented that TCM has fewer adverse side effects in the treatment of bone disease, and this was confirmed by the results of the CCK-8 assay on BMSCs in this study.[13,41] And a clinical cohort study found that the likelihood of THA for people aged 30-59, which was the age group with the highest incidence of non-traumatic ONFH, decreased dramatically after receiving adjuvant TCM therapy.[15] In addition, there was also a consistent finding in the basic research on ONFH, that is, TCM could promote the secretion of osteogenic factors associated with human BMSCs by reducing inflammation and oxidative stress.[3] It is not difficult to conclude from the combination of these basic and clinical research results that TCM is an effective treatment for ONFH with a great deal of potential and energy.

According to Shu et al.[20] and Sun et al.,[21] JTG, which is a member of the TCM family, has been shown to improve calcium and phosphorus metabolism, promote fracture healing, reduce pain, and reduce the risk of adverse events. This product is beneficial due to its composition, which includes bone collagen polypeptides, bone morphogenetic proteins, and polysaccharides that are very similar to natural tiger bone. An evaluation of the therapeutic effects of Chinese and Western medicines, conducted by Zhao et al.[39] showed that some TCM medicines (particularly JTG capsules) were more effective than the Western medicines (such as calcium and alendronate sodium tablets) in improving the BMD at the lumber spine (L2-L4). As a result of its remarkable success in treating bone loss with JTG as well as its only minor gastrointestinal side effects, this drug has been included in the 2017 treatment guidelines for osteoporosis in China.[42] Due to the range of indications for JTG, it has not been used in the clinic as a first-line treatment for ONFH. However, a meta-analysis of randomized controlled trials by Zhang et al.[43] found that the combination of core decompression and oral TCM may have more pronounced effects in the treatment of early-stage ONFH. Despite this, the occurrence and development of ONFH are often caused by many factors such as hemoglobin diseases, autoimmune diseases, and idiopathic diseases, therefore a comprehensive exploration of the

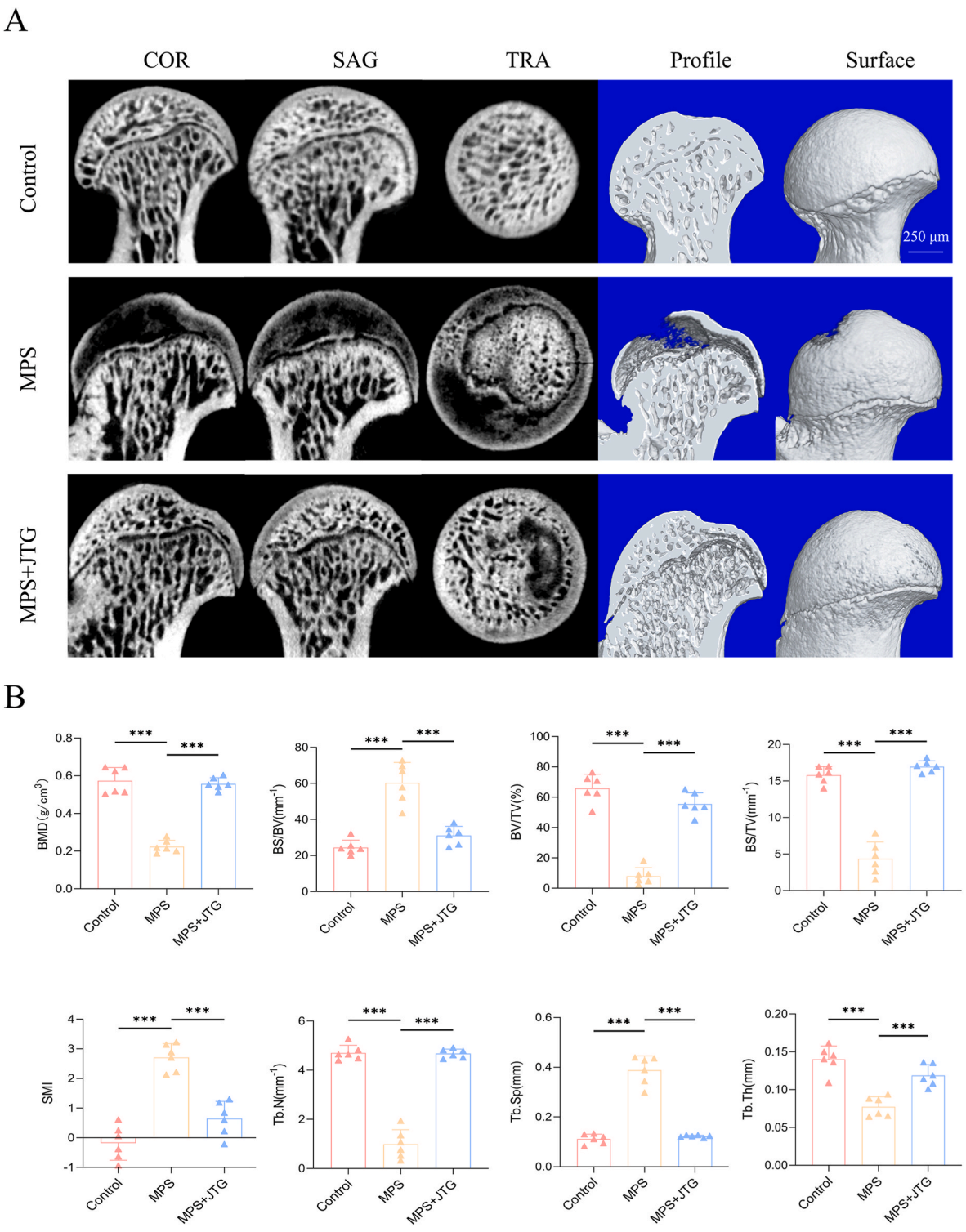

Fig. 3. Micro-CT scanning and quantitative analysis of the femoral head of rats. A) 2D and 3D images of femoral heads were divided to depict intervention and observation perspectives, which indicated that JTG was effective in alleviating bone loss associated with MPS. B) Quantitative analysis of subchondral bone for BMD, BV/TV, BS/BV, BS/TV, Tb.Pf, SMI, Tb.Th, and Tb.Sp. The data were represented as the mean ± SD (n = 6 per group, $p < 0.05$; *$p < 0.01$; ***$p < 0.001$ relative to the MPS group).

mechanism of JTG in the treatment of GC-ONFH requires a multi-angle and multi-level assessment in the future.[44]

Synthesizing the inspiring results of this study, it was not difficult to find that BMD and other osteogenic parameters of the trabecula in the subchondral bone area of the femoral head were indeed increased overall in MPS + JTG group compared with the MPS group. In addition, the femoral head of JTG-treated rats showed a higher degree of mineralization, a lower percentage of lacunae, and a smaller distribution of osteoclasts in the given staining on femoral head tissue sections, indicating transposition of necrotic areas in accordance with a comprehensive report proposing the mechanism of action of JTG.[20] The changes in these detection indices confirmed that JTG was effective in affecting

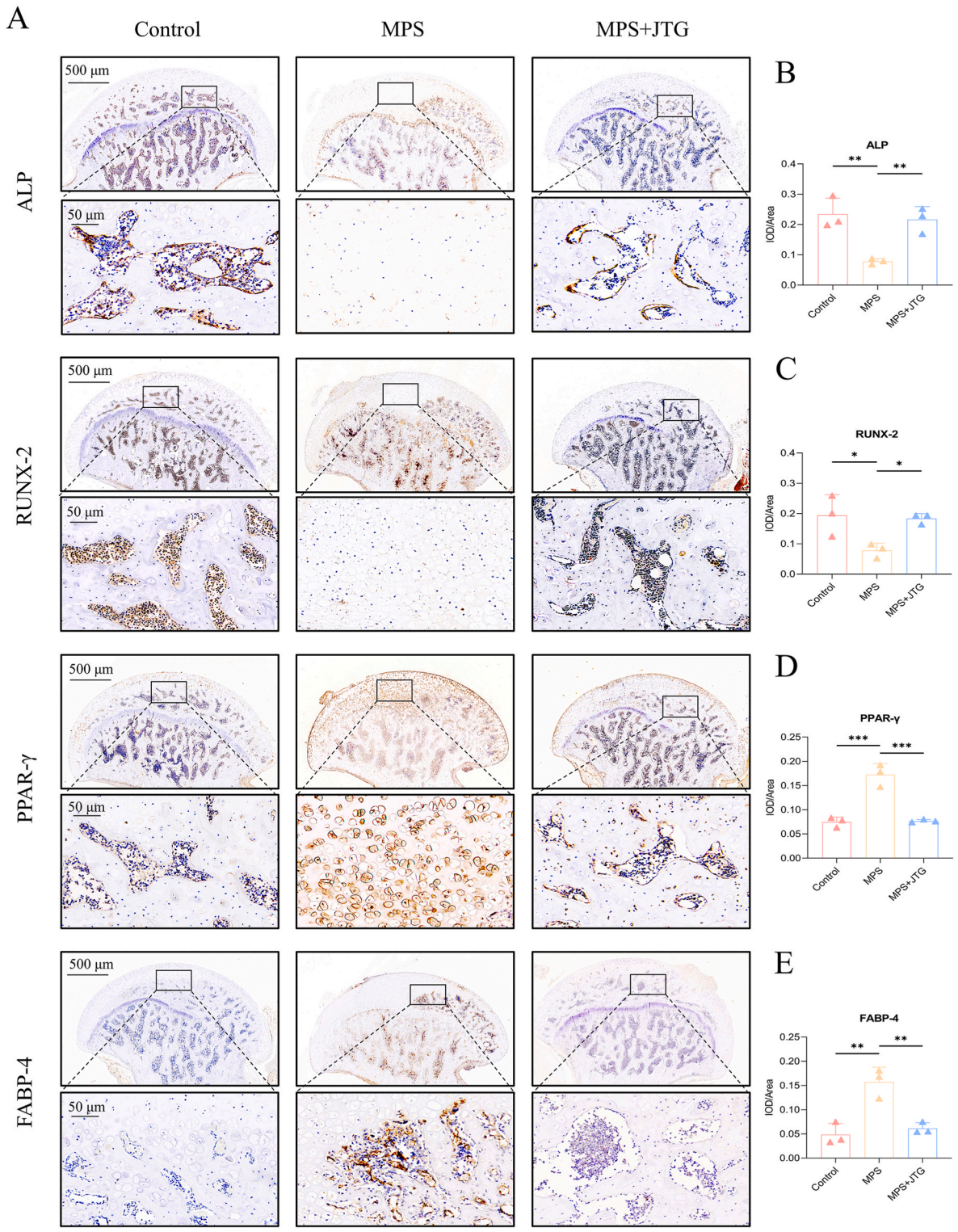

Fig. 4. IHC staining of the femoral heads of rats. A) Protein expression levels of osteogenic indices (ALP and RUNX-2) were significantly increased after JTG treatment compared with MPS-treated groups, whereas adipogenic indices (PPAR-γ and FABP-4) were reversed. B-E) Quantitative analyses of integrated option density (IOD) in selected areas of each group, and all data of each indicator were represented as mean ± SD (n = 3 per group, $p < 0.05$; *$p < 0.01$; ***$p < 0.001$ relative to the MPS group).

bone substance at the tissue level, and as such may be considered for use in the treatment of early-stage clinical GC-ONFH patients in the future.

Additionally, previous studies have shown that GC can activate osteoclasts by increasing their activity and causing inflammation, leading to a significant loss of bone mass.[45,46] Similarly, experiments by Zhuang et al.[19] showed that JTG inhibited subchondral bone remodeling, thereby delaying early OA by regulating osteoclast differentiation. Given that, apart from verifying the effect of JTG on osteoclasts in vivo at this stage, we speculate that there should be a close relationship between JTG, osteoclasts and GC-ONFH.

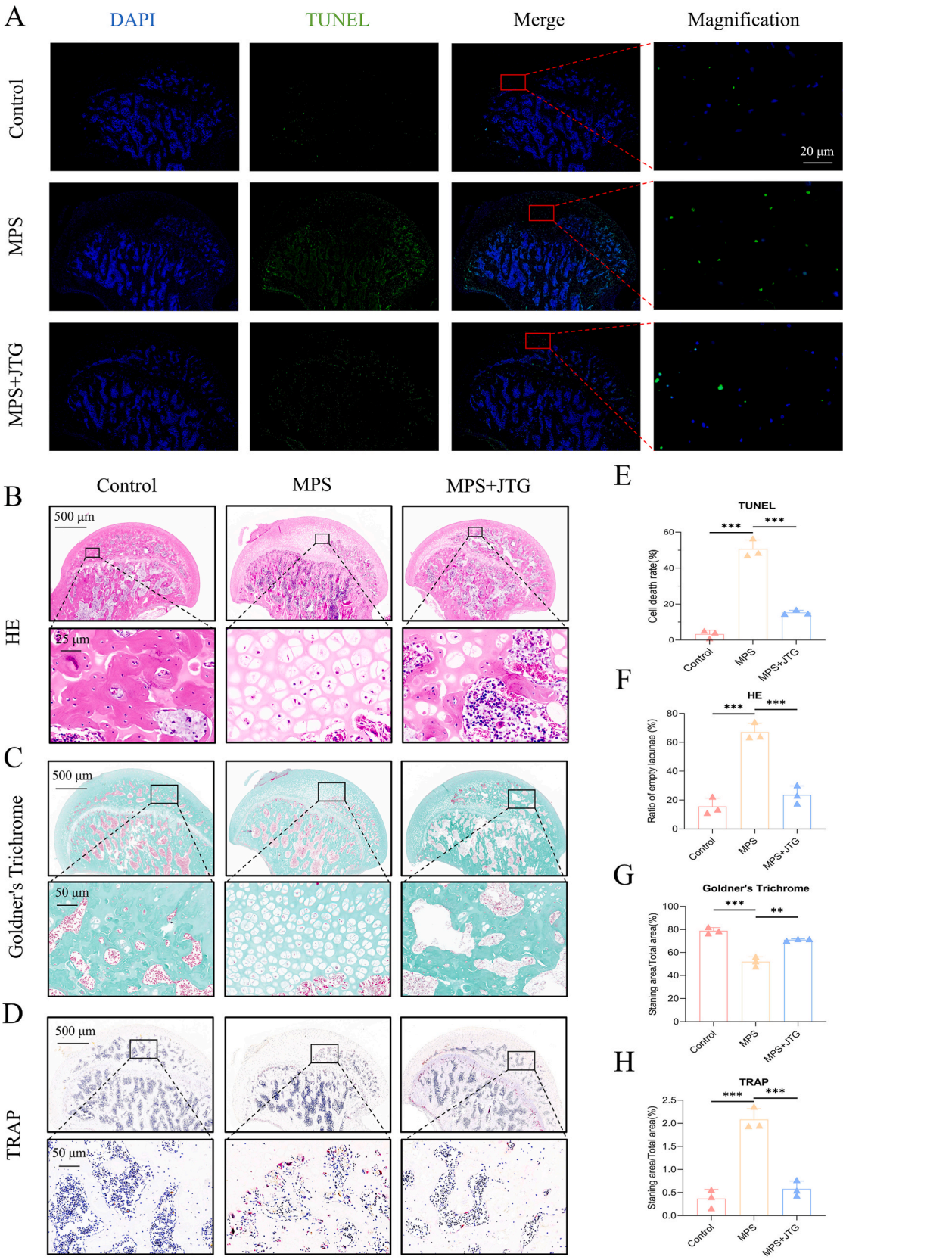

Fig. 5. TUNEL immunofluorescence and histological staining of the femoral head of rats. A) The TUNEL results demonstrated that JTG + MPS groups had a significantly lower number of apoptotic cells (green staining) than those in MPS groups. B-D) In histological HE, Goldner's Trichrome and TRAP staining, it was determined that the femoral heads treated with JTG had a lower number of empty lacunae, a higher level of mineralization (green staining) and a smaller number of osteoclasts (red staining) than those processed with MPS. E-H) Quantitative analyses of each assay were represented as the mean ± SD (n = 3 per group, $p < 0.05$; *$p < 0.01$; ***$p < 0.001$ relative to the MPS group).

As precursors of osteoblasts with multi-directional differentiation potential, BMSCs play a crucial role in enhancing bone growth, repair, and hemostasis.[47,48] Based on the results of the apoptosis and proliferation assays conducted in vitro, the addition of JTG significantly increased the lifespan and activity of BMSCs compared to DEX alone. This suggested that early-stage GC-ONFH treatment with JTG may help reverse cell deterioration.

The ratio of osteoblasts and adipocytes in BMSCs has a significant impact on bone formation as these represent the two primary directions of differentiation for BMSCs. Related reports have confirmed that RUNX-2 and PPAR-γ are the most representative master regulators of BMSCs in the process of osteogenesis and adipogenesis. They have an antagonistic relationship in the normal development of bone. Specially, high-expression of RUNX-2 and low-expression of PPAR-γ were more conducive to bone growth under the control of Wnt/β-catenin 30,49,50. Currently, activation of the Wnt/β-catenin pathway has been widely reported in studies related to the osteogenic differentiation of BMSCs[3,51,52]; coincidentally, a number of studies have shown that autophagy is activated during the osteogenic differentiation of BMSCs.[53–55] A deeper exploration of the relationship between the two factors was found that activating autophagy can degrade the YAP (Yes-associated protein) partner protein in BMSCs, thereby promoting nuclear translocation of β-catenin protein from the cytoplasm.[55] In our study, a significant increase in the content of β-catenin protein in the nucleus of BMSCs was also found, which also suggested that the promotive effect of JTG on the osteogenesis of BMSCs may be co-existed with the activation of autophagy.

Regarding osteogenic differentiation, RUNX-2 was a master regulator in the early stages of differentiation and was at the intersection of several osteogenic related signal pathways; it exhibited high levels of expression in osteoblast lineage cells, particularly pre-osteoblasts.[3,56,57] The decrease in RUNX-2 observed in this experiment, which was supported by evidence that GC could act as an antagonist to RUNX-2, suggested that GC has the ability to inhibit RUNX-2.[7] An additional marker of osteogenesis is the transcription of ALP, which is controlled by RUNX-2 and catalyzes the hydrolysis of organic phosphate in the extracellular matrix during the early stages of osteogenesis.[3,4,58] As previously reported in the literature, ALP has the ability to increase the cell vitality of bone cells, and its level can be used to assess the health and functioning of osteoblasts.[59,60]

Regarding adipogenesis differentiation, PPAR-γ, which was a key component of the PPAR pathway, could promote the uptake of fatty acids, the formation of triglycerides, and the storage of lipid droplets, which contributed PPAR-γ to become a marker of lipid content in the body.[61] Considered as a dangerous factor, the results of He et al.[50] showed that increased PPAR-γ activity has adverse effects on skeletal homeostasis by inhibiting the osteogenic differentiation and bone formation. Similarly, in the past, it was found that levels of PPAR-γ would gradually increase with the progression of GC-ONFH; and PPAR-γ downregulation can also promote the osteogenic differentiation of BMSCs to some extent, which helps alleviate the progress of early-stage GC-ONFH.[12,62] Additionally, FABP-4 has a crucial role in adipocyte formation by acting as a carrier protein for fatty acids.[63,64] Identified as an adipokine secreted by adipocytes and macrophages, FABP4 plays an important role in the development of lipid metabolism disorders, such as type-2 diabetes, coronary atherosclerosis, and fatty liver.[65] According to the findings of this study, the levels of expression of relevant target proteins, mRNA, and IHC staining were consistent with the mainstream views.

There is impossible to separate bone growth from blood supply, and the lack of research on vascularization in the necrosis area of the femoral head has become the primary weakness of this research. Aside from its effect on BMSCs and related differentiated cells, previous studies have shown that GC may reduce the number of nutrient vessels in the femoral head and cause a decrease in blood flow.[7,66] After a great deal of extensive research, growing evidence showed that the death of endocrine cells (ECs) was a significant factor in the pathological progression of GC-ONFH.[67,68] A number of studies conducted previously have found that Chinese herbs can promote angiogenesis and improve circulation reconstruction in ischemic regions of ONFH by activating blood rheology, which can help JTG treat GC-ONFH by increasing blood flow to the affected area.[16] Increasingly, type-H vessels characterized by endothelial markers CD31 and endomucin ($CD31^{hi}EMCN^{hi}$) have gained increased attention due to the deeper investigation of avascular necrosis of the femoral head in recent years.[69] There has been a great deal of research showing that type-H vessels are strongly linked to osteogenesis, compared to type-L vessels with low expression of $CD31^{hi}EMCN^{hi}$, and the number and function of type-H vessels are noticeably downregulated in osteoporosis cases.[70,71] Using fluorescent staining, Gao et al.[72] identified a large number of type-H vessels in human femoral head specimens, and this number decreased with increasing age. In the rat experiment conducted by Lane et al.,[73] it was found that the expression of $CD31^{hi}EMCN^{hi}$ was decreased in significant amounts in GC-ONFH models. These findings further suggested that there was a close relationship between GC-ONFH and type-H vessels, and provided some theoretical support for further improving the mechanism of JTG in the treatment of GC-ONFH with type-H blood vessels in the future.

5. Conclusion

Ultimately, this study establishes for the first time that JTG can promote osteogenesis and inhibit adipogenesis by affecting the activity of BMSCs, which may help to stop early-stage GC-ONFH progression in vitro and in vivo. In this regard, JTG may be an attractive candidate as a potential pharmacotherapeutic agent for early-stage GC-ONFH due to its protective properties.

Funding

This work was supported by the University Natural Science Research Project of Anhui Province (No. KJ2018A0662) and Scientific Research Funding of Anhui Medical University (No. 2022xkj163).

Declaration of competing interest

All authors state that they have no conflicts of interest.

References

1. Zheng LZ, Wang JL, Xu JK, et al. Magnesium and vitamin C supplementation attenuates steroid-associated osteonecrosis in a rat model. *Biomaterials*. 2020;238, 119828.
2. Zhou D, Chen YX, Yin JH, et al. Valproic acid prevents glucocorticoid-induced osteonecrosis of the femoral head of rats. *Int J Mol Med*. 2018;41:3433–3447.
3. Chen XJ, Shen YS, He MC, et al. Polydatin promotes the osteogenic differentiation of human bone mesenchymal stem cells by activating the BMP2-Wnt/beta-catenin signaling pathway. *Biomed Pharmacother*. 2019;112, 108746.
4. Fang B, Wang D, Zheng J, et al. Involvement of tumor necrosis factor alpha in steroid-associated osteonecrosis of the femoral head: friend or foe? *Stem Cell Res Ther*. 2019;10:5.
5. Buttgereit F. Views on glucocorticoid therapy in rheumatology: the age of convergence. *Nat Rev Rheumatol*. 2020;16:239–246.
6. Venkatesh B, Finfer S, Cohen J, et al. Adjunctive glucocorticoid therapy in patients with septic shock. *N Engl J Med*. 2018;378:797–808.
7. Zhang YL, Yin JH, Ding H, Zhang W, Zhang CQ, Gao YS. Vitamin K2 prevents glucocorticoid-induced osteonecrosis of the femoral head in rats. *Int J Biol Sci*. 2016; 12:347–358.
8. Zhao J, Ma XL, Ma JX, et al. TET3 mediates alterations in the epigenetic marker 5hmC and akt pathway in steroid-associated osteonecrosis. *J Bone Miner Res*. 2017; 32:319–332.
9. Huang Z, Cheng C, Cao B, et al. Icariin protects against glucocorticoid-induced osteonecrosis of the femoral head in rats. *Cell Physiol Biochem*. 2018;47:694–706.
10. Tao SC, Yuan T, Rui BY, Zhu ZZ, Guo SC, Zhang CQ. Exosomes derived from human platelet-rich plasma prevent apoptosis induced by glucocorticoid-associated endoplasmic reticulum stress in rat osteonecrosis of the femoral head via the Akt/Bad/Bcl-2 signal pathway. *Theranostics*. 2017;7:733–750.
11. Wang G, Wang F, Zhang L, Yan C, Zhang Y. miR-133a silencing rescues glucocorticoid-induced bone loss by regulating the MAPK/ERK signaling pathway. *Stem Cell Res Ther*. 2021;12:215.

12. Xu HH, Li SM, Fang L, et al. Platelet-rich plasma promotes bone formation, restrains adipogenesis and accelerates vascularization to relieve steroids-induced osteonecrosis of the femoral head. *Platelets*. 2021;32:950–959.
13. Cui D, Zhao D, Wang B, et al. Safflower (Carthamus tinctorius L.) polysaccharide attenuates cellular apoptosis in steroid-induced avascular necrosis of femoral head by targeting caspase-3-dependent signaling pathway. *Int J Biol Macromol*. 2018;116:106–112.
14. Xu Y, Jiang Y, Xia C, Wang Y, Zhao Z, Li T. Stem cell therapy for osteonecrosis of femoral head: opportunities and challenges. *Regen Ther*. 2020;15:295–304.
15. Yeh YA, Chiang JH, Wu MY, et al. Association of traditional Chinese medicine therapy with risk of total hip replacement in patients with nontraumatic osteonecrosis of the femoral head: a population-based cohort study. *Evid Based Complement Alternat Med 2019*. 2019, 5870179.
16. Li CG, Shen L, Yang YP, Xu XJ, Shuai B, Ma C. Effects of Modified Qing'e Pill (,) on expression of adiponectin, bone morphogenetic protein 2 and coagulation-related factors in patients with nontraumatic osteonecrosis of femoral head. *Chin J Integr Med*. 2017;23:183–189.
17. Jiang Y, Liu C, Chen W, Wang H, Wang C, Lin N. Tetramethylpyrazine enhances vascularization and prevents osteonecrosis in steroid-treated rats. *BioMed Res Int*. 2015;2015, 315850.
18. Suntornsaratoon P, Charoenphandhu N, Krishnamra N. Fortified tuna bone powder supplementation increases bone mineral density of lactating rats and their offspring. *J Sci Food Agric*. 2018;98:2027–2034.
19. Zhuang C, Wang Z, Chen W, Wang H, Tian B, Lin H. Jintiange capsules ameliorate osteoarthritis by modulating subchondral bone remodeling and protecting cartilage against degradation. *Front Pharmacol*. 2021;12, 762543.
20. Shu LJ, Zhang JY. Effect of artificial tiger bone powder (Jintiange capsule(R)) on vertebral height ratio, cobb's angle, bone mineral density, and visual analog score. *Orthop Surg*. 2022;14:427–434.
21. Sun J, Yang XG, Hu YC. Efficacy of Jintiange capsules in the treatment of osteoporosis: a network meta-analysis. *Orthop Surg*. 2019;11:176–186.
22. Peng X, Ma Y, Wang Q, et al. Serum amyloid A correlates with the osteonecrosis of femoral head by affecting bone metabolism. *Front Pharmacol*. 2021;12, 767243.
23. Ren Y, Song X, Tan L, et al. A review of the pharmacological properties of psoralen. *Front Pharmacol*. 2020;11, 571535.
24. Reggio A, Rosina M, Palma A, et al. Adipogenesis of skeletal muscle fibro/adipogenic progenitors is affected by the WNT5a/GSK3/beta-catenin axis. *Cell Death Differ*. 2020;27:2921–2941.
25. Soleimani M, Nadri S. A protocol for isolation and culture of mesenchymal stem cells from mouse bone marrow. *Nat Protoc*. 2009;4:102–106.
26. Zhou M, Xi J, Cheng Y, et al. Reprogrammed mesenchymal stem cells derived from iPSCs promote bone repair in steroid-associated osteonecrosis of the femoral head. *Stem Cell Res Ther*. 2021;12:175.
27. Zheng LZ, Wang JL, Kong L, et al. Steroid-associated osteonecrosis animal model in rats. *J Orthop Translat*. 2018;13:13–24.
28. Shen Y, Wang N, Zhang Q, et al. Jin-Tian-Ge ameliorates ovariectomy-induced bone loss in rats and modulates osteoblastogenesis and osteoclastogenesis in vitro. *Chin Med*. 2022;17:78.
29. Bouxsein ML, Boyd SK, Christiansen BA, Guldberg RE, Jepsen KJ, Muller R. Guidelines for assessment of bone microstructure in rodents using micro-computed tomography. *J Bone Miner Res*. 2010;25:1468–1486.
30. Yu H, Zhu D, Liu P, et al. Osthole stimulates bone formation, drives vascularization and retards adipogenesis to alleviate alcohol-induced osteonecrosis of the femoral head. *J Cell Mol Med*. 2020;24:4439–4451.
31. Cohen-Rosenblum A, Cui Q. Osteonecrosis of the femoral head. *Orthop Clin N Am*. 2019;50:139–149.
32. Yang Q, Yin W, Chen Y, et al. Betaine alleviates alcohol-induced osteonecrosis of the femoral head via mTOR signaling pathway regulation. *Biomed Pharmacother*. 2019;120, 109486.
33. Yu H, Liu P, Zhu D, et al. Chrysophanic acid shifts the differentiation tendency of BMSCs to prevent alcohol-induced osteonecrosis of the femoral head. *Cell Prolif*. 2020;53, e12871.
34. Wang L, You X, Zhang L, Zhang C, Zou W. Mechanical regulation of bone remodeling. *Bone Res*. 2022;10:16.
35. Zhang XL, Shi KQ, Jia PT, et al. Effects of platelet-rich plasma on angiogenesis and osteogenesis-associated factors in rabbits with avascular necrosis of the femoral head. *Eur Rev Med Pharmacol Sci*. 2018;22:2143–2152.
36. Cao F, Liu G, Wang W, et al. Combined treatment with an anticoagulant and a vasodilator prevents steroid-associated osteonecrosis of rabbit femoral heads by improving hypercoagulability. *BioMed Res Int*. 2017;2017, 1624074.
37. Haumer A, Bourgine PE, Occhetta P, Born G, Tasso R, Martin I. Delivery of cellular factors to regulate bone healing. *Adv Drug Deliv Rev*. 2018;129:285–294.
38. Mao L, Jiang P, Lei X, et al. Efficacy and safety of stem cell therapy for the early-stage osteonecrosis of femoral head: a systematic review and meta-analysis of randomized controlled trials. *Stem Cell Res Ther*. 2020;11:445.
39. Zhao J, Zeng L, Wu M, et al. Efficacy of Chinese patent medicine for primary osteoporosis: a network meta-analysis. *Compl Ther Clin Pract*. 2021;44, 101419.
40. Xu W, Xing FJ, Dong K, et al. Application of traditional Chinese medicine preparation in targeting drug delivery system. *Drug Deliv*. 2015;22:258–265.
41. Wei X, Xu A, Shen H, Xie Y. Qianggu capsule for the treatment of primary osteoporosis: evidence from a Chinese patent medicine. *BMC Compl Alternative Med*. 2017;17:108.
42. Yan Z, Li J, He X, et al. Jintiange capsule may have a positive effect on pain relief and functional activity in patients with knee osteoarthritis: a meta-analysis of randomized trials. *Evid Based Complement Alternat Med*. 2021;2021, 7908429.
43. Zhang Q, Yang F, Chen Y, et al. Chinese herbal medicine formulas as adjuvant therapy for osteonecrosis of the femoral head: a systematic review and meta-analysis of randomized controlled trials. *Medicine (Baltim)*. 2018;97, e12196.
44. Zhao D, Zhang F, Wang B, et al. Guidelines for clinical diagnosis and treatment of osteonecrosis of the femoral head in adults (2019 version). *J Orthop Translat*. 2020;21:100–110.
45. Chen K, Liu Y, He J, et al. Steroid-induced osteonecrosis of the femoral head reveals enhanced reactive oxygen species and hyperactive osteoclasts. *Int J Biol Sci*. 2020;16:1888–1900.
46. Ngo D, Beaulieu E, Gu R, et al. Divergent effects of endogenous and exogenous glucocorticoid-induced leucine zipper in animal models of inflammation and arthritis. *Arthritis Rheum*. 2013;65:1203–1212.
47. Chia W, Liu J, Huang YG, Zhang C. A circular RNA derived from DAB1 promotes cell proliferation and osteogenic differentiation of BMSCs via RBPJ/DAB1 axis. *Cell Death Dis*. 2020;11:372.
48. Zhu B, Xue F, Li G, Zhang C. CRYAB promotes osteogenic differentiation of human bone marrow stem cells via stabilizing beta-catenin and promoting the Wnt signalling. *Cell Prolif*. 2020;53, e12709.
49. Rauch A, Haakonsson AK, Madsen JGS, et al. Osteogenesis depends on commissioning of a network of stem cell transcription factors that act as repressors of adipogenesis. *Nat Genet*. 2019;51:716–727.
50. He HP, Gu S. The PPAR-gamma/SFRP5/Wnt/beta-catenin signal axis regulates the dexamethasone-induced osteoporosis. *Cytokine*. 2021;143, 155488.
51. Zhao SJ, Kong FQ, Jie J, et al. Macrophage MSR1 promotes BMSC osteogenic differentiation and M2-like polarization by activating PI3K/AKT/GSK3beta/beta-catenin pathway. *Theranostics*. 2020;10:17–35.
52. Zhou P, Li Y, Di R, et al. H19 and Foxc2 synergistically promotes osteogenic differentiation of BMSCs via Wnt-beta-catenin pathway. *J Cell Physiol*. 2019;234:13799–13806.
53. Garavaglia B, Vallino L, Ferraresi A, et al. Butyrate inhibits colorectal cancer cell proliferation through autophagy degradation of β-catenin regardless of APC and β-catenin mutational status. *Biomedicines*. 2022;10.
54. Vidoni C, Ferraresi A, Secomandi E, et al. Autophagy drives osteogenic differentiation of human gingival mesenchymal stem cells. *Cell Commun Signal*. 2019;17:98.
55. Li L, Yang S, Xu L, et al. Nanotopography on titanium promotes osteogenesis via autophagy-mediated signaling between YAP and beta-catenin. *Acta Biomater*. 2019;96:674–685.
56. Komori T. Regulation of proliferation, differentiation and functions of osteoblasts by Runx2. *Int J Mol Sci*. 2019;20.
57. Balla B, Sarvari M, Kosa JP, et al. Long-term selective estrogen receptor-beta agonist treatment modulates gene expression in bone and bone marrow of ovariectomized rats. *J Steroid Biochem Mol Biol*. 2019;188:185–194.
58. Hu N, Feng C, Jiang Y, Miao Q, Liu H. Regulative effect of mir-205 on osteogenic differentiation of bone mesenchymal stem cells (BMSCs): possible role of SATB2/runx2 and ERK/MAPK pathway. *Int J Mol Sci*. 2015;16:10491–10506.
59. Llorente-Pelayo S, Docio P, Lavin-Gomez BA, et al. Modified serum ALP values and timing of apparition of knee epiphyseal ossification centers in preterm infants with cholestasis and risk of concomitant metabolic bone disease of prematurity. *Nutrients*. 2020;12.
60. Yokoi Y. Osteoblast-like cell proliferation, ALP activity and photocatalytic activity on sintered anatase and rutile titanium dioxide. *Materials*. 2021;14.
61. Montaigne D, Butruille L, Staels B. PPAR control of metabolism and cardiovascular functions. *Nat Rev Cardiol*. 2021;18:809–823.
62. Bai H, Chen T, Lu Q, Zhu W, Zhang J. Gene expression profiling of the bone trabecula in patients with osteonecrosis of the femoral head by RNA sequencing. *J Biochem*. 2019;166:475–484.
63. Wang T, Teng S, Zhang Y, Wang F, Ding H, Guo L. Role of mesenchymal stem cells on differentiation in steroid-induced avascular necrosis of the femoral head. *Exp Ther Med*. 2017;13:669–675.
64. Yu Z, Fan L, Li J, Ge Z, Dang X, Wang K. Lithium chloride attenuates the abnormal osteogenic/adipogenic differentiation of bone marrow-derived mesenchymal stem cells obtained from rats with steroid-related osteonecrosis by activating the beta-catenin pathway. *Int J Mol Med*. 2015;36:1264–1272.
65. Zhang C, Chiu KY, Chan BPM, et al. Knocking out or pharmaceutical inhibition of fatty acid binding protein 4 (FABP4) alleviates osteoarthritis induced by high-fat diet in mice. *Osteoarthritis Cartilage*. 2018;26:824–833.
66. Huang C, Wen Z, Niu J, Lin S, Wang W. Steroid-induced osteonecrosis of the femoral head: novel insight into the roles of bone endothelial cells in pathogenesis and treatment. *Front Cell Dev Biol*. 2021;9, 777697.
67. Gao Y, Zhu H, Wang Q, Feng Y, Zhang C. Inhibition of PERK signaling prevents against glucocorticoid-induced endotheliocyte apoptosis and osteonecrosis of the femoral head. *Int J Biol Sci*. 2020;16:543–552.
68. Gao Y, Zhu H, Yang F, Wang Q, Feng Y, Zhang C. Glucocorticoid-activated IRE1alpha/XBP-1s signaling: an autophagy-associated protective pathway against endotheliocyte damage. *Am J Physiol Cell Physiol*. 2018;315:C300–C309.
69. Peng Y, Wu S, Li Y, Crane JL. Type H blood vessels in bone modeling and remodeling. *Theranostics*. 2020;10:426–436.
70. Kusumbe AP, Ramasamy SK, Adams RH. Coupling of angiogenesis and osteogenesis by a specific vessel subtype in bone. *Nature*. 2014;507:323–328.

71. Xu R, Yallowitz A, Qin A, et al. Targeting skeletal endothelium to ameliorate bone loss. *Nat Med*. 2018;24:823–833.
72. Gao F, Mao T, Zhang Q, Han J, Sun W, Li Z. H subtype vascular endothelial cells in human femoral head: an experimental verification. *Ann Palliat Med*. 2020;9:1497–1505.
73. Lane NE, Mohan G, Yao W, et al. Prevalence of glucocorticoid induced osteonecrosis in the mouse is not affected by treatments that maintain bone vascularity. *BoneKEy Rep*. 2018;9:181–187.